PCCP

Accepted Manuscript

This article can be cited before page numbers have been issued, to do this please use: L. Zhang, A. Cheruvathur, C. Biz, M. Fianchini and J. Gracia, *Phys. Chem. Chem. Phys.*, 2019, DOI: 10.1039/C8CP07832G.

ROYAL SOCIETY OF CHEMISTRY

rsc.li/pccp

ARTICLE

Ferromagnetic Ligand Holes in Cobalt Perovskite Electrocatalysts as Essential Factor for High Activity Towards Oxygen Evolution

View Article Online
DOI: 10.1039/C8CP07832G

Received 00th January 20xx,
Accepted 00th January 20xx

DOI: 10.1039/x0xx00000x
www.rsc.org/

Ling Zhang,[a] Ajin Cheruvathur,[a] Chiara Biz,[b] Mauro Fianchini,[c] Jose Gracia*[d]

The definition of the interplay between chemical composition, electro-magnetic configuration and catalytic activity requires a rational study of the orbital physics behind active materials. Apart from Coulomb forces, quantum spin exchange interactions (QSEI) are part of the potentials that differentiate the activity of magnetic oxides in electron transfer reactions, strongly correlated electrocatalysts. Ferromagnetic (FM) cobalt oxides can show low overpotentials for the oxygen evolution reaction (OER); and the $La_{1-X}Sr_XCoO_{3-\delta}$ ($0 \le X \le 1$) family of perovskites is a good ground to gain understanding of the electronic interactions in strongly correlated catalysts. In this case, Sr-doping raises the OER activity, the conductivity and increasing FM spin moments. The efficiency of electrocatalysts based on Earth-abundant ***3d***-transition metals correlate with the interrelated factors: mild-boding energies, the reduction of the electronic repulsions because of the QSEI in the open-shells, and with enhanced spin delocalization in FM orderings. The epitome of the outstanding OER activity of $SrCoO_{3-\delta}$ is the accumulation of FM holes in the ***3d-2p*** bonds, including the ligand orbitals, thus facilitating spin-selected charge transport and production of triplet O_2 moieties, from the oxidation of diamagnetic precursors. Spin-polarized oxygen atoms in the lattice can participate in O-O coupling and extrusion of O_2 in a Mars-Van Krevelen mechanistic fashion. We show that the stabilizing FM QSEI decrease the adsorption and activation energies during oxygen evolution; and spin-dependent potentials are part of the factors that govern the catalytic activity of magnetic compositions: *spintro-catalysis*.

Introduction

Water oxidation enables conversion of electricity into storable hydrogen, needed for clean energy and a sustainable economy. In water electrolysis, the oxygen evolution reaction (OER) is the rate limiting step of the overall process. Therefore much attention has devoted to understand the rationale behind triplet state O_2 evolution in order to develop active, stable and abundant catalysts that accelerate it[1]. In 1980 Matsumoto and co-workers examined the OER activity of the $La_{1-X}Sr_XFe_{1-Y}Co_YO_{3-\delta}$ ($0 \le X \le 1$ and $0 \le Y \le 1$) family of perovskites in alkaline solution[2]; even though the group could not synthesise the ($Co^{\sim 4+}$) $SrCoO_{3-\delta}$ composition, they predicted that it will show the lower overpotentials. The $La_{0.2}Sr_{0.8}Fe_{0.2}Co_{0.8}O_{3-\delta}$ structure was obtained by Matsumoto as an excellent and stable electrocatalyst for OER; similar compositions and oxidation states typically lead to good catalysts[3,4,5]. In the smaller $La_{1-X}Sr_XCoO_{3-\delta}$ group, $SrCoO_{3-\delta}$ shows the optimum OER kinetic and is, in fact, one of the best catalysts[6,7].

In 1984 Bockris and Otagawa described the electrocatalytic activity of perovskite oxides in terms of molecular orbital theory[8]; they show that the antibonding (AB) ***3d***-metal orbitals directed towards the ligands (O) overlap with the lobes of the reactants forming AB σ*-type orbitals, ***e_g-2p*** shells in octahedral coordination. The authors explained that the catalysts having occupied ***e_g-2p*** levels achieve high rates of oxygen evolution due to mild bonding between the catalyst and the intermediates. Separately, Goodenough has established the foundations of the theoretical understanding of the electronic and magnetic transitions in metal oxides[9,10]. These works have been key to derive the significant influence of quantum spin exchange interactions (QSEI) in the orbital chemistry of magnetic catalysts, also known as spintro-catalysis[11]. Due to the impact of QSEI in compositions with open-shell configurations,[12] conventional electronic analysis in heterogenous catalysis like the d-band centre model / band theory[13] are insufficient to describe the highly-correlated electrons; and then lead to rough approximations for the catalytic activity of materials based-on Earth-abundant magnetic elements. As in spintronics, the spins of many electrons can act together, affect the magnetic and electronic properties of a material, and influence significantly its catalytic behaviour.

QSEI reduce the electronic repulsions and are key for charge mobility in magnetic systems[12]. A ferromagnetic (FM) conduction band indicates that the physics of the itinerant electrons is significantly influenced by Fermi holes, a fundamental requirement for optimal electrocatalysts based on ***3d***-metals[11,14]. By looking carefully, we can see examples where magnetic structures associate overall with active heterogeneous catalysis. FM oxides show better activity than Pt in the oxidation of nitrous oxide (NO has doublet ground state)[15,16], FM nitrides improve ammonia synthesis[17], or Co doping in MoS_2 induces FM[18] and enhances the activity in various reactions. In addition of particular interest for electrocatalysis, inter-atomic FM orderings leads to favourable spin-charge transport, avoiding antiferromagnetic (AFM) electronic localization.[12] Fully AFM insulators like $LaCrO_3$ or $LaFeO_3$ are poor oxygen catalysts[19,20]. Spin selection in polarized density of states facilitates the oxidation/reduction of triplet state O_2.[21,22] Nature has evolved excellent magnetic catalysts from abundant ***3d***-metals, e.g. during photosynthesis[23], via engineering QSEI.

In a broad context, the rationalisation of the orbital physics in magnetic structures is important in theoretical heterogenous catalysis, because it will allow to study activities across the whole periodic table based on the interplay between chemical composition, and electronic configuration. Successful catalytic design based on orbital occupation[14,24] may proceed from the rigorous analysis of the quantum chemistry[25]. In **the** $La_{1-X}Sr_XCo_YO_{3-\delta}$ family **two ends for the OER activity can be defined: $LaCoO_3$ as the less active and $SrCoO_{3-\delta}$ as the most efficient.** The orbital physics behind the intrinsic activity of $SrCoO_{3-\delta}$ is unknown, as well as the effect of the iron ions in compositions like $La_{0.2}Sr_{0.8}Fe_{0.2}Co_{0.8}O_{3-\delta}$. **Also,** the specific orbital configuration of $LaCoO_3$ at room temperature is controversial, because three spin states representing the ***3d-2p*** AB-orbitals in octahedral coordination, $t_{2g}^6e_g^0$ (low spin, LS), $t_{2g}^4e_g^2$ (high spin, HS) and $t_{2g}^5e_g^1$ (intermediate spin, IS), are accessible for the Co^{3+}-O bonds. $LaCoO_3$ presents the following, not fully understood, electronic transitions as a function of temperature[26,27]:

- 0 K < T < 35 K: bulk cobalt cations are preferentially in the Low-Spin (LS) $t_{2g}^6e_g^0$ diamagnetic state.
- 35 K < T < 110 K: cobalt cations coexist in intermediate-spin (IS) $t_{2g}^5e_g^1$ and high-spin (HS) $t_{2g}^4e_g^2$ configurations with a ratio of LS/(HS + IS) > 0.5.

[a] *SynCat@Beijing, Synfuels China Technology Co. Ltd., Leyuan South Street II, No. 1, Yanqi Economic Development Zone C#, Huairou District, 101407 Beijing (China)*
[b] *Department of Inorganic and Organic Chemistry, Universitat Jaume I, Av. Vicente Sos Baynat s/n, E-12071 Castellón de la Plana, Spain*
[c] *Institute of Chemical Research of Catalonia (ICIQ), The Barcelona Institute of Technology, Avgda Països Catalans 16, 43007 Tarragona, Spain*
[d] *MagnetoCat SL, General Polavieja 9 3I, 03012 Alicante, Spain*

- 110 K < T < 350 K: a mixture of approximately 50% LS and 50 % HS cobalt cations forms a semi-conductive paramagnetic (PM) phase.
- 350 K < T < 650 K: the semi-conductive phase coexists with a metallic phase, possibly due to the presence of IS cations. An insulator-to-metal transition occurs near 450 K.

The phases of $LaCoO_3$ accommodate diverse Jahn-Teller (JT) distortions as the XRD patterns indicate[28,29]. Below 90 K (Tab. 1) the experimental Co-O distances are similar, 1.918-1.934 Å, and shorter than those at higher temperatures[28].

Different electronic configurations coexist in cobalt-based oxides; the present manuscript explains via DFT(GGA+U) calculations the electronic structure behind the poor or good OER activity in the $La_{1-X}Sr_XFe_{1-Y}Co_YO_{3-\delta}$ series. The initial comparison between theory and experiment is based on bulk properties; and it serves to calibrate the method. Finally, we explore the mechanism for oxygen evolution on the most efficient $SrCoO_{3-\delta}$, looking for a quantification of the specific influence of QSEI in the valence open-shells in reaction steps.

Theoretical methods

We have performed periodic Density Functional Theory (DFT) calculations using VASP (Vienna Ab-initio Simulation Package), a program that combines ab-initio energy calculations with plane-wave basis sets[30–33]. The electron-ion interactions for the atoms are described by the projector augmented wave method developed by Blöchl[34,35]. The exchange-correlation energy has been calculated within the generalized gradient approximation using the Perdew-Burke-Ernzerhof functional revised for solids[36]. We used a cut-off energy of 400 eV for the expansion of the wave function into plane waves. The Monkhorst–Pack scheme has been chosen for the integration in the reciprocal space[37]. We have used the so-called DFT+U approach for the corrections accounting for the strong correlation among the electrons at the Co and Fe atoms[38]. The Hubbard +U correction is desirable in 3d-metals to consider explicitly non-local interactions between localized electrons[39]. The value of U is a constant, thus, in order to get accurate results, a structure-dependent parametrization of U is necessary[40]. An initial calibration of GGA +U method was performed in order to match the electronic configurations of the $LaCoO_3$ and $SrCoO_{3-\delta}$ catalysts. The lattice parameters for monoclinic I2/a $LaCoO_3$ were optimized using a single unit cell, 4 La, 4 Co and 12 oxygen atoms, versus U. Optimizations indicate that for U 2.0 - 2.5 the Hubbard correction is suitable to both experimental Jahn-Teller distortions[29,41] (see Table 1) and expected relative stability of competing electronic configurations[21]. The reciprocal space has been sampled with a (7x7x5) k-point grid for the ground-state optimized lattice parameters (experimental within brackets): a = 5.309 Å (5.367), b = 5.417 Å (5.433), c = 7.719 Å (7.637), β = 90.8º (91.0). The $SrCoO_{3-\delta}$ (001) slab model has lattice parameters of a = 5.333 Å, b = 5.333 Å and c = 30.0 Å and about 15 Å vacuum gap. The reciprocal space has been sampled with a (5x5x1) k-point grid. The climbing-image nudged elastic band (cNEB) method is used to determine minimum-energy paths, via 8 images and a spring constant of 5.0 eV/Å^2. All the plots and the iso-surfaces for spin densities (0.03 e$^-$/Å^3 iso-value) have been realized using VESTA[42].

Results and discussion

View Article Online
DOI: 10.1039/C8CP07832G

In our calculations, the $LaCoO_3$ ground-state has all the Co^{3+} cations in LS configuration. The $t_{2g}^6e_g^0$ structure presents no JT distortion and the predicted Co-O distance is about ~ 1.893 Å. The density of states (DOS), Fig. 1a, shows that LS $LaCoO_3$ is an insulator with a band gap of about 0.5 eV. The second most stable phase is the ¾ LS + ¼ HS configuration, Fig. 1b; the inter-atomic exchange interactions are favourably ferromagnetic, because the e_g band is overall more empty than occupied[9].

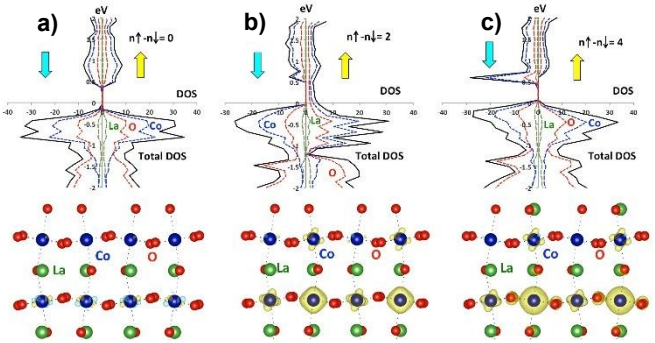

Figure 1. Top: density of states (DOS) versus energy in eV. Bottom: Spin density for the configurations a) LS, b) FM ¾ LS + ¼ IS and c) FM ¾ LS + ¼ HS. The spin density is shown in yellow and the Fermi level = 0 eV.

Table 1. Calculated and experimental $LaCoO_3$ Co-O distances (Å) and relative energies per Cobalt atom (meV/Co^{3+}) for the most stable configurations.

State		Co $\lvert\mu_B\rvert$	Co-O (Å) 1	2	3	ΔE
DIA	**LS**	0.0	1.893	1.893	1.895	0
FM	**¾ LS**	0.2	1.870	1.870	1.907	12
	¼ HS	2.8	1.908	1.944	1.945	
FM	**¾ LS**	0.2	1.885	1.894	1.898	41
	¼ IS	1.6	1.888	1.896	1.910	
FM	**½ LS**	0.5	1.867	1.881	1.883	24
	½ HS	2.8	1.884	1.964	1.970	
AFM	**½ LS**	0.0	1.871	1.883	1.887	32
	½ HS	2.8	1.883	1.971	1.974	
FM	**½ LS**	0.4	1.873	1.874	1.891	57
	¼ IS	1.6	1.864	1.905	1.907	
	¼ HS	2.8	1.895	1.954	1.955	
Experimental[29,40]						
DIA	***90 K***		*1.918*	*1.924*	*1.934*	
PM	***298 K***		*1.874*	*1.925*	*1.993*	

Both ¾ LS + ¼ HS and ¾ LS + ¼ IS structures present JT distortions on the cobalt atoms with localized magnetic moments, see Tab. 1. The DOS for ¾ LS + ¼ HS $LaCoO_3$ also has a band gap of ~0.5 eV, while ¾ LS + ¼ IS is a half-metal. This last configuration, less stable, is not detected experimentally. At room temperature $LaCoO_3$ possesses a narrow optical gap < 1.0 eV[43]; and our calculations predict a band gap of ~0.5 eV (Fig. 1a and 2). The LS $\mathbf{t_{2g}^6e_g^0}$ configuration has a band gap because of the energy difference between the fully occupied $\mathbf{t_{2g}^6}$ and the empty $\mathbf{e_g^0}$ levels; effect due to the splitting of ***3d***-shells in the crystal-field. A similar thing occurs between the fully occupied valence band in the HS $\mathbf{t_{2g}^6e_g^2}$ cobalt atoms and the conduction band. However, for IS $\mathbf{t_{2g}^5e_g^1e_g^0t_{2g}^0}$ configurations, the degenerate and semi-occupied **3d**-shells form metallic bands.

The FM ½ LS + ½ HS ordering is slightly more stable than the AFM configuration, and above 120 K entropy disorders the spins. These structures accessible at 300 K present cooperative Jahn-Teller type distortions with ~5% of maximum deviation between the average experimental distances and the calculated ones. Both LS and HS Co^{3+} atoms show localization of spin density within the ***3d***-metal and ***2p***-oxygen orbitals. This suggests the presence of a mixed valence occupations and enhanced ***3d-2p*** hybridization with the increment of on-site magnetism. Overall, the electrocatalytic activity of $LaCoO_3$ observed at room temperature is at least initially restricted by the limited charge conductivity.

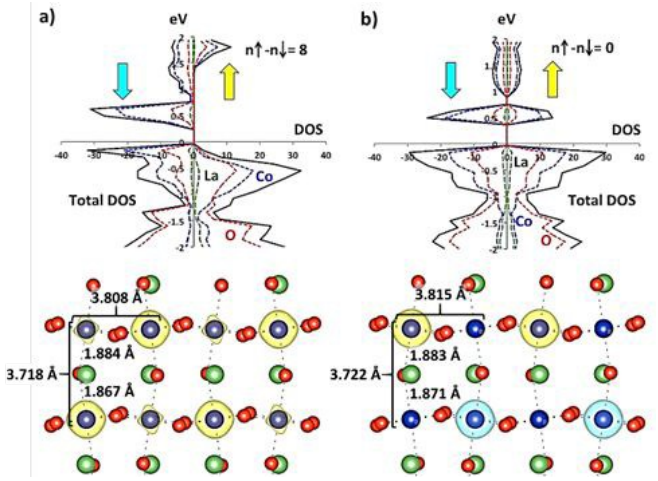

Figure 2. Top: density of states (DOS) versus energy in eV. Bottom: spin density for the Co^{3+} atoms in the two ½ LS + ½ HS accessible configurations of $LaCoO_3$ at 110 K < T < 350 K, a) FM ½ LS + ½ HS, b) AFM ½ LS + ½ HS. Different colours for the spin density on the cobalt atoms indicate a relative change in the orientation of the spins.

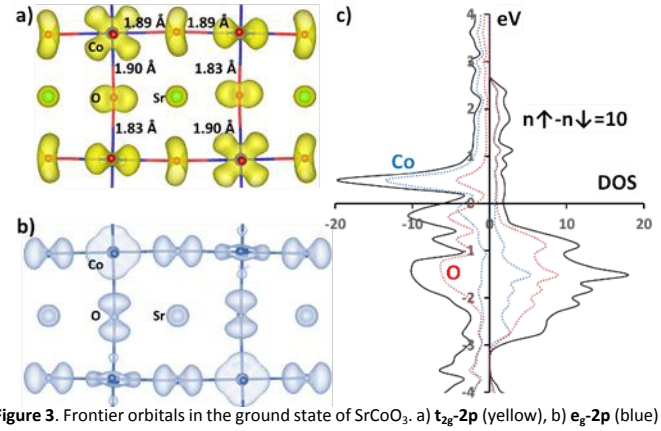

Figure 3. Frontier orbitals in the ground state of $SrCoO_3$. a) t_{2g}-**2p** (yellow), b) e_g-**2p** (blue) and c) density of states, DOS.

$SrCoO_{3-\delta}$ is a FM conductor (T_C = 305 K) with a total magnetization of ~2.5μ_B per octahedral shell[44] and a percentage of oxygen vacancies typical of Co^{4+} oxides[6]. Calculations on the $SrCoO_3$ and $SrCoO_{2.75}$ stoichiometries result in FM metallic ground states with a total spin of ~2.5μ_B within Co-O bonds, in perfect agreement with experimental data. Fig. 3 shows the conduction band constituted by the frontier t_{2g}-**2p** and e_g-**2p** orbitals, for the majority and minority of spin. The on-site QSEI in the open-shells are crucial to investigate the correct electron paring and the partial population of the AB-orbitals. The alternate orientation pattern in the adjacent orthogonal atomic ***3d***-orbitals reduces the electronic repulsions, without JT elongations and instead with some short Co-O bonds of 1.83 Å. A hypothetical AFM configuration, about 0.8 eV higher in energy from the FM configuration, recovers the JT distortions, with an elongation of some Co-O bonds to about 1.93 Å.

The admirable agreement between the GGA+U calculations and the experimental structural, electronic and magnetic properties for the two oxidation extremes, $LaCoO_3$ and $SrCoO_{3-\delta}$, indicates a high degree of confidence in the comparison with the following stoichiometries: $La_{0.75}Sr_{0.25}CoO_3$, $La_{0.5}Sr_{0.5}CoO_3$, $La_{0.25}Sr_{0.75}CoO_{3-\delta}$ and $La_{0.25}Sr_{0.75}Co_{0.75}Fe_{0.25}O_{3-\delta}$.

All the compositions in the $La_{1-X}Sr_XCoO_{3-\delta}$ family are extended FM gapless conductors apart from $LaCoO_3$[45], p-type semi-conductor. In their ground-states, the AB-eigenvectors show a concomitant increment of the ***3d-2p*** hybridization with the magnetization, which is maximum in $SrCoO_3$ (Fig. 3 and 4). The participation of the ***2p***-orbitals of the ligands in the AB-shell at the conduction band increases with the number of Fermi holes. The relative number of t_{2g}-**2p** electrons with minority spin decreases with the increasing oxidation states, and the magnetic density in the Co-O bonds growths, favoured by the QSEI.

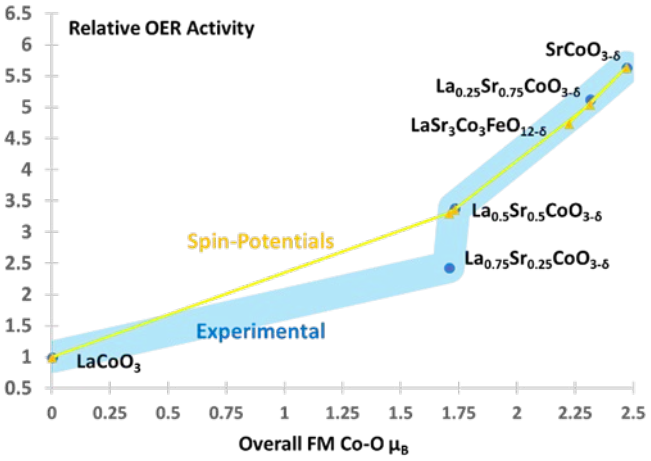

Figure 4. Experimental and predicted, obtained using Eq .1, relative OER intrinsic activity for the $La_{1-X}Sr_XCoO_{3-\delta}$ family with respect to $LaCoO_3$ in alkaline media. It indicates that increasing FM in the G.S. seems inherent to the OER activity in cobalt-based oxides.

Fig. 4 shows the trend of the accumulated FM spin-moment in Co-O bonds (in the ground state) versus the experimental relative intrinsic OER activity[6,7]; we could have also used only the spin-density on the oxygen atoms ($\boldsymbol{\mu_O^{FM}}$). The electronic structure of $La_{0.25}Sr_{0.75}Co_{0.75}Fe_{0.25}O_{3-\delta}$ shows that this material possesses the same overall average magnetization as $SrCoO_{3-\delta}$. The presence of Fe ions increases the magnetism due to their own $t_{2g}^3e_g^1$ shells, while the spin-polarization overall decreases on the Co-O AB-orbitals. Overall $La_{0.25}Sr_{0.75}Co_{0.75}Fe_{0.25}O_{3-\delta}$ has less FM ligand holes, this explains that iron atoms serve to increase the stability of the $Co^{\sim 4+}$ oxides, but not the intrinsic OER activity. The trend shown in Fig. 4 is mathematically expressed by Eq. 1, that is derived from Eq. 3 by assuming that $\Delta H_{act.st}^{(0).cat.1} \approx \Delta H_{act.st}^{(0).cat.2}$. For the $La_{1-X}Sr_XCoO_{3-\delta}$ family, $\Delta J_{QEI}^{OER} \cdot \boldsymbol{\mu_{cat.}}$ gives almost a quantitative prediction of the relative OER activity. The composition with the highest OER activity has a maximum $\boldsymbol{\mu_{cat.}^{FM}}$ value. The validity of this derivation should

View Article Online
DOI: 10.1039/C8CP07832G

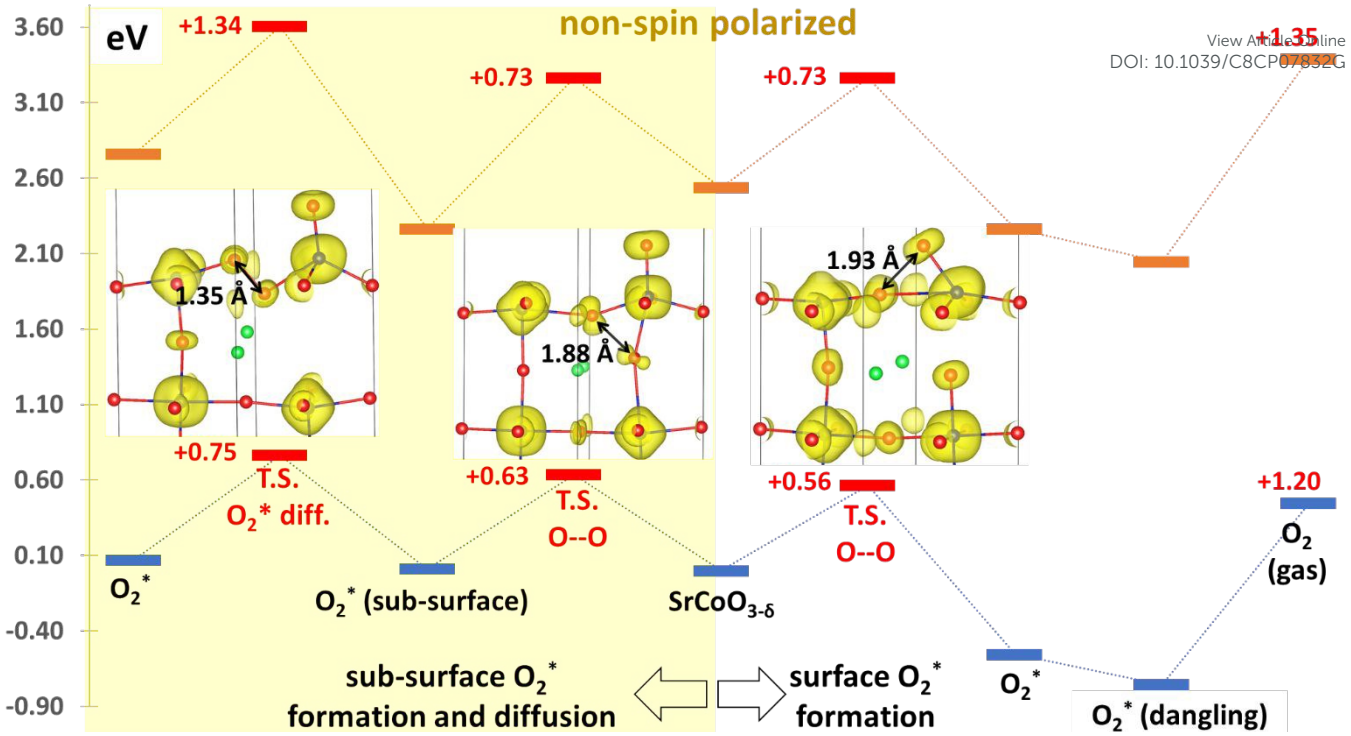

Figure 5. Thermodynamics and spin density for the formation, adsorption and desorption of an O_2 molecule over a $SrCoO_{3-\delta}$ (001) surface. Bottom right quadrant describes MvK-type surface mechanism calculated including spin polarization (QEI). Bottom left quadrant describes oxygen coupling via the mobility of sub-surface oxygen atoms, again including spin-polarisation. Top-right and top-left quadrant describe the non-spin polarised version of the same mechaniss. In all cases the spin-density of the oxygen atoms indicates spin-selection.

serve to compare the relative intrinsic OER activity of different structures and ***3d***-metals by using $\boldsymbol{\mu_O^{FM}}$.

$$\textit{Eq. 1)}\ K_{relative.OER}^{\mathrm{QSEI}} = e^{\Delta J_{QSEI}^{OER} \cdot \boldsymbol{\mu_{cat.}^{FM}}}$$

The enthalpy of any chemical event mainly depends upon three kinds of energy terms, Eq. 2. In magnetic catalysts, the additional non-classical $QSEI_{shells}^{open}$, $\Delta \boldsymbol{Exc.}_{e-e-}^{\boldsymbol{QSEI.open.shells}} \propto \Delta J_{QEI}^{OER} \cdot \boldsymbol{\mu_{cat.}}$, are part of the stabilizing potentials, and relatively as higher is their value smaller are the Coulomb terms.[14]

$$\textit{Eq. 2)}\ \Delta H_{event}^{cat.} = \Delta K_{e-}^{kinetic} + [\Delta C_{N+N+}^{rep.} + \Delta C_{e-N+}^{att.} + \Delta C_{e-e-}^{rep.}]_{Coulomb}^{classical} + \left[\Delta Exc._{e-e-}^{QSEI.closed.shells} + \Delta Exc._{e-e-}^{QSEI.open.shells}\right].$$

Cooperative $QSEI_{shells}^{open}$ are indispensable to understand magnetic catalysts, since spin-potentials are responsible of the electronic conductivity and important in the orbital interactions, but how much? Limiting our study to the formation triplet O_2, Fig. 5 shows the thermodynamic steps of two possible mechanisms over a $SrCoO_{3-\delta}$ (001) surface for oxygen evolution. We compare between hypothetical close-shell (non-spin-polarized) calculations (Fig. 5 top) and the open-shell spin-polarized mechanisms (Fig.5 bottom). QSEI reduce the energy of open-shells by a contribution of around 3±0.5 eV; this is not a trivial value. The kinetic is also significantly improved in the spin-polarized calculations, the activation barriers and the adsorption energies decrease considerably between 15% and 35% in comparison with the fictious close-shell system. The initial surface formation of an O-O bond has an activation energy of ~+0.56 eV, while the same step requires ~+0.73 eV in the non-spin polarized calculations. Fig. 5 is in agreement with the specialized GGA+U literature[46]. Moreover, calculations reveal structural discrepancies between close-shell and open shells calculations, for instance M-O bond distances vary by ~±0.1 Å.

We considered two possible pathways for O-O coupling (centre-to-left and centre-to-right): calculations of a classical surface mechanism go from the centre to the right; and a sub-surface pathway is from the centre to the left. The surface mechanism is more favourable mainly due to the restricted mobility of sub-surface O-O* units. Our observations are in line with the work of Mefford and co-workers: the group noticed the presence of bulk oxygen mobility in OER on $SrCoO_{3-\delta}$ catalysts[6]. It is also consistent with the role of lattice oxygen in the computational work of Yoo and co-workers[47].

The peculiar property of the highly oxidised mixed-valence $SrCoO_{3-\delta}$ composition is the ability to insert nucleophilic lattice oxygen towards the formation of O_2*; which after desorption, leaves concomitant oxygen vacancies. These mobile vacancies can be rapidly occupied by oxygen atoms through the diffusion of bulk atoms and by gas phase intermediates, alike. This phenomenon creates a high turnover in the numbers of the active centres at the surface[48]. Then excellent OER activities seem associated with an overall Mars-van Krevelen type mechanism that is characteristic of total oxidations[48,49].

We already knew that coupled mixed-valence spin acceptors (or donors), showing preferential FM interactions in the partially occupied AB $\boldsymbol{e_g}$***-2p*** orbitals, are good conductors and excellent oxygen spintro-catalysts[24]. Furthermore, prototypical oxides for OER are those structures with metals in a high oxidation state, and then sufficiently electronegative. Eq. 3 correlates the overall activation energy of FM catalysts with the specific influence of $QSEI_{shells}^{open}$, added via a Heisenberg type exchange term[14,22].

Eq. 3) $\Delta \boldsymbol{H}_{\boldsymbol{act.st}}^{\boldsymbol{FM.QEI}} \approx \Delta \boldsymbol{H}_{\boldsymbol{act.st}}^{(\boldsymbol{0})} - \Delta \boldsymbol{J}_{\boldsymbol{act.st}}^{\boldsymbol{FM.Exc.}} \cdot \boldsymbol{\mu}_{\boldsymbol{cat.}}^{\boldsymbol{FM}}$

Eq. 3 means that ***3d-2p*** hybridization and magnetization of the AB-eigenvectors, $\boldsymbol{\mu}_{\boldsymbol{cat.}} = \boldsymbol{\mu}_{\boldsymbol{3d}} + \boldsymbol{\mu}_{\boldsymbol{2p}}$, is an important design factor in every technology involving oxygen production and evolution[24]. Eq. 3 also explains that the trends for ***3d***-metals do not follow the simple parabolic behaviours postulated by band theory[49]. For instance, Mott insulators governed by antiferromagnetic (AFM) superexchange interactions are less active oxygen electro-catalysts indicating $-\Delta \boldsymbol{J}_{\boldsymbol{act.st}}^{\boldsymbol{AFM.Exc.}} \cdot \boldsymbol{\mu}_{\boldsymbol{cat.}}^{\boldsymbol{AFM}} > \boldsymbol{0}$.

Magnetism is not a simple catalytic descriptor, on the contrary, it reflects multiple interrelated electronic properties. These factors are spin-dependent charge conductivity, oxidation state, ligand holes, intermediate bonding, reduction of the electronic repulsions. Since the nature of the magnetic coupling (whether AFM or FM) is related to electrostatic potentials, covalency and electron occupancy, spin-potentials strongly influence OER activity, and provide a physical sense to the statistical evaluation of descriptors done in the group of Shao-Horn[50]. In comparison with other theoretical descriptors in oxygen electrocatalysis, the recent calculations by Tripkovic and co-workers on the series $LaMO_3$ (M = Cr, Mn, Fe, Co, Ni) show the ineffectiveness of trying to differentiate the electrocatalytic activities of magnetic systems simply from the binding energies of species like O* and OH*[51].

We report the suitability of the GGA+U method in the description of the electronic structure of $La_{1-X}Sr_XFe_{1-Y}Co_YO_{3-\delta}$ compositions; what it is not a surprise since GGA+U is a well-established approach to try to capture the physics of strongly correlated catalysts[52]. Computational studies on correlated oxides without Hubbard corrections are more in error when calculating reactions. In addition, if spin polarization is not even included on magnetic oxides the reported values are too inaccurate, what lead to multiple errors like the overestimation of the activity of insulating materials.

Conclusions

Are quantum spin exchange interactions a fundamental electronic factor in the catalytic activity of magnetic oxides? Yes, they are.

We have seen that the inter-atomic magnetic moment accumulated in the bonds of Co-based perovskites relates with charge conductivity, Fermi holes in the ligands, spin-selection and moderate binding energies. Consequently, $QSEI_{shells}^{open}$ are indispensable to understand the behaviour of magnetic materials, and for determining their electrocatalytic activity and selectivity. Expected conclusion considering that are materials of interest in spintronics.

The increment of oxidation state for Co from $LaCo^{III}O_3$ to $SrCo^{IV}O_{3-\delta}$ induces an improvement of O_2 release, in addition to good spin-conductivity, consequently an enhancement of the OER activity indicated by maximum $\boldsymbol{\mu}_{\boldsymbol{cat.}}^{\boldsymbol{FM}}$ and $\boldsymbol{\mu}_{\boldsymbol{O}}^{\boldsymbol{FM}}$. In the highly active $SrCoO_{3-\delta}$, the initial formation of the O-O bond is governed by spin-transfer from the ligands to the electronegative metal atoms (Co), in a mechanism guided by $QSEI_{shells}^{open}$.

Conflicts of interest

The authors declare no conflicts of interest.

View Article Online
DOI: 10.1039/C8CP07832G

Acknowledgements

Syngaschem BV and MagnetoCat SL gratefully acknowledge significant funding from Synfuels China Technology, Co, Ltd, Beijing-Huairou. CB and JG acknowledge and thank the Servei D'Informatica and the University Jaume I for the provision of the computational resources and Prof. Armando Beltrán Flors of the Quimica Teorica y Computacional group for the useful training.

Notes and references

1. Sapountzi FM, Gracia J, Weststrate CJ, Fredriksson HOA, Niemantsverdriet JW. Electrocatalysts for the generation of hydrogen, oxygen and synthesis gas. *Prog Energy Combust Sci*. 2017;58:1-35. doi:10.1016/j.pecs.2016.09.001.
2. Matsumoto Y, Sato E. Oxygen evolution on La1−xSrxMnO3 electrodes in alkaline solutions. *Electrochim Acta*. 1979;24(4):421-423. doi:10.1016/0013-4686(79)87030-9.
3. Grimaud A, May KJ, Carlton CE, et al. Double perovskites as a family of highly active catalysts for oxygen evolution in alkaline solution. *Nat Commun*. 2013;4(May):2439. doi:10.1038/ncomms3439.
4. Zhu Y, Zhou W, Chen Z-G, et al. SrNb0.1Co0.7Fe0.2O3−δ Perovskite as a Next-Generation Electrocatalyst for Oxygen Evolution in Alkaline Solution. *Angew Chemie Int Ed*. 2015;54(13):3897-3901. doi:10.1002/anie.201408998.
5. Lee D-G, Gwon O, Park H-S, et al. Conductivity-Dependent Completion of Oxygen Reduction on Oxide Catalysts. *Angew Chemie Int Ed*. 2015;54(52):15730-15733. doi:10.1002/anie.201508129.
6. Mefford JT, Rong X, Abakumov AM, et al. Water electrolysis on La1−xSrxCoO3−δ perovskite electrocatalysts. *Nat Commun*. 2016;7:11053. doi:10.1038/ncomms11053.
7. Cheng X, Fabbri E, Nachtegaal M, et al. Oxygen Evolution Reaction on La1–xSrxCoO3 Perovskites: A Combined Experimental and Theoretical Study of Their Structural, Electronic, and Electrochemical Properties. *Chem Mater*. 2015;27(22):7662-7672. doi:10.1021/acs.chemmater.5b03138.
8. Bockris JO, Otagawa T. The Electrocatalysis of Oxygen Evolution on Perovskites. *J Electrochem Soc*. 1984;131(2):290. doi:10.1149/1.2115565.
9. Goodenough JB. Electronic and ionic transport properties and other physical aspects of perovskites. *Reports Prog Phys*. 2004;67(11):1915-1993. doi:10.1088/0034-4885/67/11/R01.
10. Goodenough JB. An interpretation of the magnetic properties of the perovskite-type mixed crystals La1-xSrxCoO3 *J Phys Chem Solids*. 1958;6(2-3):287-297. doi:10.1016/0022-3697(58)90107-0.
11. Gracia J, Sharpe R, Munarriz J. Principles determining the activity of magnetic oxides for electron transfer reactions. *J Catal*. 2018;361:331-338. doi:10.1016/j.jcat.2018.03.012.
12. Dagotto E. Complexity in Strongly Correlated Electronic Systems. *Science* 2005;309(5732):257-262. doi:10.1126/science.1107559.
13. Nørskov JK. Covalent effects in the effective-medium

theory of chemical binding: Hydrogen heats of solution in the 3d metals. *Phys Rev B*. 1982;26(6):2875-2885. doi:10.1103/PhysRevB.26.2875.

14. Gracia J. Spin dependent interactions catalyse the oxygen electrochemistry. *Phys Chem Chem Phys*. 2017;19(31):20451-20456. doi:10.1039/C7CP04289B.
15. Wang W, McCool G, Kapur N, et al. Mixed-Phase Oxide Catalyst Based on Mn-Mullite (Sm, Gd)Mn2O5 for NO Oxidation in Diesel Exhaust. *Science*. 2012;337(August):832-835. doi:10.1126/science.1225091.
16. Kim CH, Qi G, Dahlberg K, Li W. Strontium-doped perovskites rival platinum catalysts for treating NOx in simulated diesel exhaust. *Science*. 2010;327(5973):1624-1627. doi:10.1126/science.1184087.
17. Munarriz J, Polo V, Gracia J. On the Role of Ferromagnetic Interactions in Highly Active Mo-Based Catalysts for Ammonia Synthesis. *ChemPhysChem*. 2018;19(21):2843-2847. doi:10.1002/cphc.201800633.
18. Xiang Z, Zhang Z, Xu X, Zhang Q, Wang Q, Yuan C. Room-temperature ferromagnetism in Co doped MoS2 sheets. *Phys Chem Chem Phys*. 2015;17(24):15822-15828. doi:10.1039/C5CP01509J.
19. Kremenić G, Nieto JML, Tascón JMD, Tejuca LG. Chemisorption and catalysis on LaMO3 oxides. *J Chem Soc Faraday Trans 1 Phys Chem Condens Phases*. 1985;81(4):939. doi:10.1039/f19858100939.
20. Han B, Risch M, Lee Y-L, Ling C, Jia H, Shao-Horn Y. Activity and stability trends of perovskite oxides for oxygen evolution catalysis at neutral pH. *Phys Chem Chem Phys*. 2015;17(35):22576-22580. doi:10.1039/C5CP04248H.
21. Lim T, Niemantsverdriet JWH, Gracia J. Layered Antiferromagnetic Ordering in the Most Active Perovskite Catalysts for the Oxygen Evolution Reaction. *ChemCatChem*. 2016;8(18):2968-2974. doi:10.1002/cctc.201600611.
22. Gracia J, Munarriz J, Polo V, et al. Analysis of the Magnetic Entropy in Oxygen Reduction Reactions Catalysed by Manganite Perovskites. *ChemCatChem*. 2017;9(17):3358-3363. doi:10.1002/cctc.201700302.
23. Jiao Y, Sharpe R, Lim T, Niemantsverdriet JWH, Gracia J. Photosystem II Acts as a Spin-Controlled Electron Gate during Oxygen Formation and Evolution. *J Am Chem Soc*. 2017;139(46):16604-16608. doi:10.1021/jacs.7b07634.
24. Sharpe R, Munarriz J, Lim T, et al. Orbital Physics of Perovskites for the Oxygen Evolution Reaction. *Top Catal*. 2018;61(3-4):267-275. doi:10.1007/s11244-018-0895-4.
25. Sharpe R, Lim T, Jiao Y, Niemantsverdriet JWH, Gracia J. Oxygen Evolution Reaction on Perovskite Electrocatalysts with Localized Spins and Orbital Rotation Symmetry. *ChemCatChem*. 2016;8(24):3762-3768. doi:10.1002/cctc.201600835.
26. Señarís-Rodríguez MA, Goodenough JB. LaCoO3 Revisited. *J Solid State Chem*. 1995;116(2):224-231.
27. Asai K, Yokokura O, Nishimori N, et al. Neutron-scattering study of the spin-state transition and magnetic correlations in La1-XSrXCoO3 (X=0 and 0.08). *Phys Rev B*. 1994;50(5):3025-3032. doi:10.1103/PhysRevB.50.3025.
28. Maris G, Ren Y, Volotchaev V, Zobel C, Lorenz T, Palstra TTM. Evidence for orbital ordering in LaCoO3. *Phys Rev B*. 2003;67(22):224423. doi:10.1103/PhysRevB.67.224423.
29. Haas O, Struis RPWJ, McBreen JM. Synchrotron X-ray absorption of LaCoO3 perovskite. *J Solid State Chem*. 2004. doi:10.1016/j.jssc.2003.10.004.
30. Kresse G, Furthmüller J. Efficient iterative schemes for ab initio total-energy calculations using a plane-wave basis set. *Phys Rev B - Condens Matter Mater Phys*. 1996;54(16):11169-11186. doi:10.1103/PhysRevB.54.11169.
31. Kresse G, Furthmüller J. Efficiency of ab-initio total energy calculations for metals and semiconductors using a plane-wave basis set. *Comput Mater Sci*. 1996;6(1):15-50.
32. Kresse G, Hafner J. Ab initio molecular dynamics for liquid metals. *Phys Rev B*. 1993;47(1):558-561. doi:10.1103/PhysRevB.47.558.
33. Kresse G, Hafner J. Ab initio molecular-dynamics simulation of the liquid-metal–amorphous-semiconductor transition in germanium. *Phys Rev B*. 1994;49(20):14251-14269. doi:10.1103/PhysRevB.49.14251.
34. Blöchl PE. Projector augmented-wave method. *Phys Rev B*. 1994;50(24):17953-17979. doi:10.1103/PhysRevB.50.17953.
35. Kresse G, Joubert D. From ultrasoft pseudopotentials to the projector augmented-wave method. *Phys Rev B*. 1999;59(3):1758-1775. doi:10.1103/PhysRevB.59.1758.
36. Perdew JP, Ruzsinszky A, Csonka GI, et al. Restoring the Density-Gradient Expansion for Exchange in Solids and Surfaces. *Phys Rev Lett*. 2008;100(13):136406. doi:10.1103/PhysRevLett.100.136406.
37. Monkhorst HJ, Pack JD. Special points for Brillouin-zone integrations. *Phys Rev B*. 1976;13(12):5188-5192.
38. Dudarev SL, Botton GA, Savrasov SY, Humphreys CJ, Sutton AP. Electron-energy-loss spectra and the structural stability of nickel oxide: An LSDA+U study. *Phys Rev B - Condens Matter Mater Phys*. 1998;57(3):1505-1509. doi:10.1103/PhysRevB.57.1505.
39. Nilsson F, Aryasetiawan F. Electronic structure of strongly correlated materials: from one-particle to many-body theory. *Mater Res Express*. 2017;4(3):034001. doi:10.1088/2053-1591/aa5fa1.
40. Hsu H, Umemoto K, Cococcioni M, Wentzcovitch R. First-principles study for low-spin LaCoO3 with a structurally consistent Hubbard U. *Phys Rev B - Condens Matter Mater Phys*. 2009;79(12):1-9. doi:10.1103/PhysRevB.79.125124.
41. Maris G, Ren Y, Volotchaev V, Zobel C, Lorenz T, Palstra TTM. Evidence for orbital ordering in LaCoO3. *Phys Rev B*. 2003;67:224423. doi:10.1103/PhysRevB.67.224423.
42. Momma K, Izumi F. VESTA 3 for three-dimensional visualization of crystal, volumetric and morphology data. *J Appl Crystallogr*. 2011;44(6):1272-1276. doi:10.1107/S0021889811038970.
43. Arima T, Tokura Y, Torrance JB. Variation of optical gaps in perovskite-type 3d transition-metal oxides. *Phys Rev B*. 1993;48(23):17006-17009.
44. Long Y, Kaneko Y, Ishiwata S, Taguchi Y, Tokura Y. Synthesis of cubic SrCoO3 single crystal and its anisotropic magnetic and transport properties. *J Phys Condens Matter*. 2011;23(24):245601. doi:10.1088/0953-8984/23/24/245601.
45. Kozuka H, Yamada H, Hishida T, Yamagiwa K, Ohbayashi K, Koumoto K. Electronic transport properties of the perovskite-type oxides La1-xSrxCoO3±δ. *J Mater Chem*. 2012;22(38):20217. doi:10.1039/c2jm34613c.
46. Wang L, Maxisch T, Ceder G. Oxidation energies of transition metal oxides within the GGA+U framework. *Phys*

Journal Name ARTICLE

View Article Online
DOI: 10.1039/C8CP07832G

Rev B. 2006;73(19):195107. doi:10.1103/PhysRevB.73.195107.

47. Yoo JS, Liu Y, Rong X, Kolpak AM. Electronic Origin and Kinetic Feasibility of the Lattice Oxygen Participation During the Oxygen Evolution Reaction on Perovskites. *J Phys Chem Lett*. 2018;9(7):1473-1479. doi:10.1021/acs.jpclett.8b00154.
48. Bielanski A, Haber J. *Oxygen in Catalysis*. (Haber J, ed.). New York: M. Dekker; 1991.
49. Doornkamp C, Ponec V. The universal character of the Mars and Van Krevelen mechanism. *J Mol Catal A Chem*. 2000;162(1-2):19-32. doi:10.1016/S1381-1169(00)00319-8.
50. Hong WT, Welsch RE, Shao-Horn Y. Descriptors of Oxygen-Evolution Activity for Oxides: A Statistical Evaluation. *J Phys Chem C*. 2016;120(1):78-86. doi:10.1021/acs.jpcc.5b10071.
51. Tripkovic V, Hansen HA, Garcia-Lastra JM, Vegge T. Comparative DFT+U and HSE Study of the Oxygen Evolution Electrocatalysis on Perovskite Oxides. *J Phys Chem C*. 2018;122(2):1135-1147. doi:10.1021/acs.jpcc.7b07660.
52. Wang L, Maxisch T, Ceder G. Oxidation energies of transition metal oxides within the GGA+U framework. *Phys Rev B*. 2006;73(19):195107. doi:10.1103/PhysRevB.73.195107.